

# Time reverse modeling of low-frequency microtremors: Application to hydrocarbon reservoir localization

Brian Steiner,<sup>1</sup> Erik H. Saenger,<sup>1,2</sup> and Stefan M. Schmalholz<sup>1</sup>

Received 20 September 2007; revised 4 December 2007; accepted 27 December 2007; published 7 February 2008.

[1] Time reverse modeling is applied to synthetic and real low-frequency microtremors measured at the Earth surface with synchronized seismometers. In contrast to previous time-reverse applications, no single event or first arrival time identification is applied for microtremor localization. Synthetic low-frequency microtremors are numerically generated within a small underground area and modeled with a finite-difference algorithm simulating two-dimensional elastic wave propagation. Time reverse modeling using synthetic microtremors shows that small underground source areas can be accurately located. Different source characteristics which emit mainly P-waves or S-waves vertically influence the localization accuracy. Time reverse modeling is applied to two real microtremor data sets acquired 16 months apart above known oil reservoirs nearby Voitsdorf, Austria, to investigate whether spectral anomalies observed above the reservoirs originate from the reservoirs. Time reverse modeling indicates that low-frequency microtremor signals originate from the reservoir locations and provides a possible method for reservoir localization. **Citation:** Steiner, B., E. H. Saenger, and S. M. Schmalholz (2008), Time reverse modeling of low-frequency microtremors: Application to hydrocarbon reservoir localization, *Geophys. Res. Lett.*, 35, L03307, doi:10.1029/2007GL032097.

## 1. Introduction

[2] Novel methods to improve hydrocarbon reservoir detection are a keen interest for the petroleum industry. One method is passive low-frequency spectral analysis [e.g., Graf *et al.*, 2007]. Spectra of passively acquired ground motion signals (i.e. microtremors) measured with three-component seismometers are tested for anomalies within the low-frequency range, usually 1 Hz to 10 Hz. Several field studies have shown that systematic spectral anomalies measured within a grid of seismometers at the Earth surface are related to underground hydrocarbon reservoirs [Dangel *et al.*, 2003; Akrawi and Bloch, 2006; Graf *et al.*, 2007]. Figure 1 illustrates two real data examples. A possible explanation of the measured spectral anomalies is resonant oscillation of oil within the porous reservoir, where the resonance frequency of the oil is transferred to the solid rock matrix [Graf *et al.*, 2007]. Following this approach the reservoir acts as a secondary source. However, whether the spectral anomalies really originate from the reservoir is unresolved.

<sup>1</sup>Geological Institute, ETH Zurich, Zurich, Switzerland.

<sup>2</sup>Spectraseis AG, Zurich, Switzerland.

[3] In this study, time reverse modeling (TRM) applied to measured microtremors provides evidence signals exhibiting the spectral anomalies originate from hydrocarbon reservoirs. TRM is applied in several fields of science such as Medical and Earth Sciences [e.g., Fink, 1999]. Prior time reverse studies focus on filtering single events out of recordings of low S/N-ratio [e.g., Kao and Shan, 2004] or on spatial and temporal accuracy of single event localization [e.g., Gajewski and Tessmer, 2005; Mehta and Snieder, 2006]. A technique similar to TRM is interferometric seismic imaging, a generalized version of daylight imaging by Claerbout [1968], which locates reflections using correlated passive seismic data [e.g., Schuster *et al.*, 2004; Wapenaar *et al.*, 2004]. Furthermore, special cross-correlation applications filter a seismic source out of a complex media and noisy surrounding [e.g., Garnier, 2005]. In general, these methods either locate a single event or require a first arrival time identification. Therefore, none of these methods is applicable to microtremors that are used for passive low-frequency spectral analysis, because no single events and first arrival times are present.

[4] In this study, TRM is applied to synthetic microtremors and to real seismic data acquired over reservoirs nearby Voitsdorf, Austria. Synthetic microtremors generated by two-dimensional finite difference (FD) simulations of elastic wave propagation are used for numerical TRM to determine if a well defined small source area can be located. Three numerical simulations illustrate the impact of different source characteristics on localization accuracy. Finally, TRM is applied to two real microtremor data sets, acquired 16 months apart, recorded with synchronized seismometers above well understood reservoirs. TRM results of both data sets demonstrate that subsurface reservoir locations may be located using this method.

## 2. Method and Synthetic Feasibility Study

[5] Numerical modeling generates synthetic microtremors. The numerical modeling algorithm used for forward and reverse modeling of seismic wave propagation solves the two-dimensional (2D) elastic wave equation. The wave equation is transformed into the first order velocity-stress formulation [Virieux, 1986] with rectangular numerical grid. The rotated staggered grid FD technique by Saenger *et al.* [2000] is applied. All computations are performed with second order spatial FD operators and with second order explicit time update. The top of the model is a free surface and wave absorbing layers are implemented at the three other boundaries to simulate non-reflecting boundaries [Clayton and Engquist, 1977].

[6] A heterogeneous velocity model (Figure 2a) with homogeneous and isotropic model units is used to generate

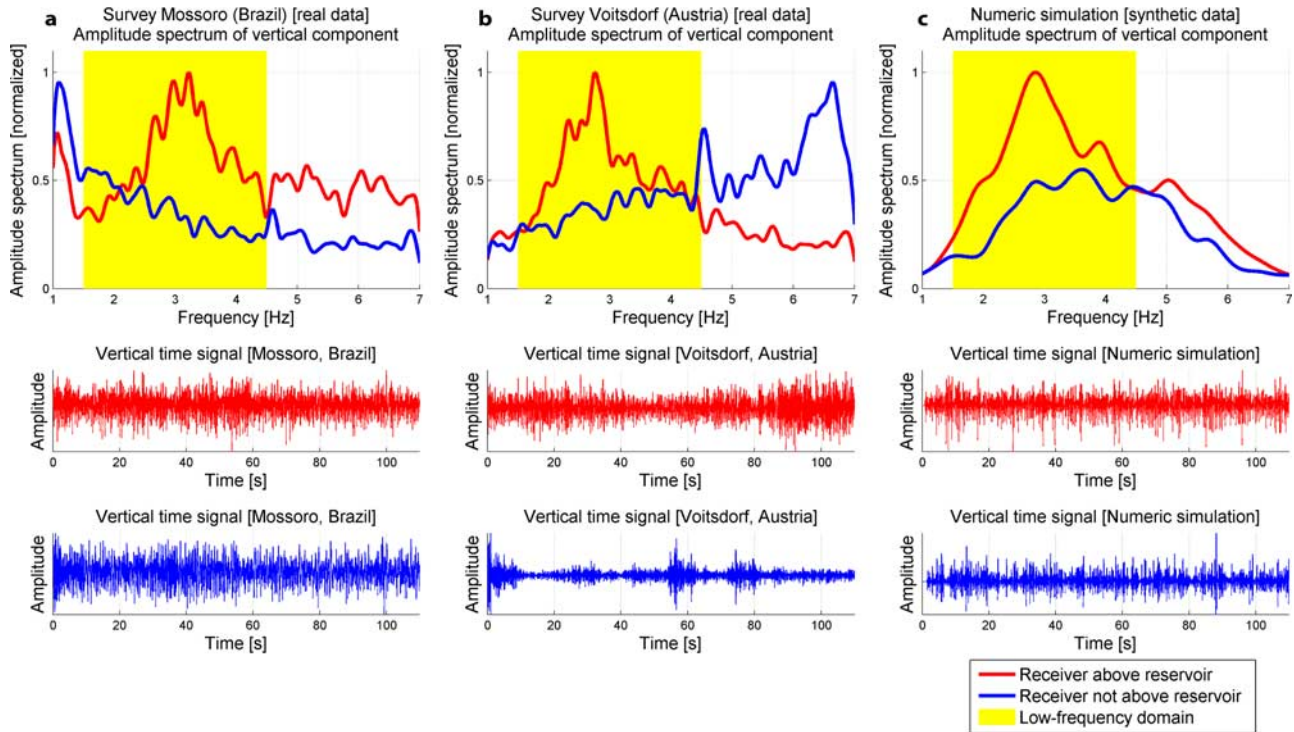


**Figure 1.** Amplitude spectra and the corresponding vertical particle velocity versus time signals recorded at the surface from field surveys in (a) Brazil and (b) Austria. Higher spectral amplitudes are observed above the reservoir. The synthetic microtremors (c) are similar to the real data examples.

microtremors. The FD grid is 9 km wide and 3 km deep and consists of 901 horizontal and 301 vertical nodes with spacing of 10 m. The wave absorbing layers are 500 m thick. The ten units have a density  $\rho = 2000 \text{ kg/m}^3$  and their P-wave velocities  $v_P$  increase in 200 m/s steps from 1200 m/s (top layer) to 3000 m/s (bottom layer). The basal model unit represents a crystalline basement with  $\rho = 3000 \text{ kg/m}^3$  and  $v_P = 6000 \text{ m/s}$ . For the line-shaped heterogeneity  $\rho = 2000 \text{ kg/m}^3$  and  $v_P = 2000 \text{ m/s}$ . The model reservoir area close to the middle of the model domain is about 50 m thick and 2000 m wide with  $\rho = 2000 \text{ kg/m}^3$  and  $v_P = 2500 \text{ m/s}$ . All S-wave velocities are about a factor 1.4 smaller than the P-wave velocities of the same model unit.

[7] Forward modeling generates continuous microtremor signals similar to natural ones. Continuous microtremors are generated by applying 574 individual, short-time low-frequency sources with a fundamental frequency ranging between 1.5 Hz and 4.5 Hz (i.e. second derivative of Gaussian). These sources are randomly distributed within the zone representing the reservoir area (black line, Figures 2a–2d), randomly distributed during the 180 second numerical simulation and provide a microtremor signal whose spectra are similar to the ones of the natural microtremors (Figure 1). The numerical time step is  $2.9 \cdot 10^{-4}$  seconds. The horizontal and vertical particle velocities are recorded through time with 11 virtual seismometers at the model surface (Figure 2a).

[8] Three numerical forward simulations with different source types generate synthetic microtremors. In Simulation 1 the applied source function generates P-waves only by adding specific values to the normal stresses in the stress

equations (i.e. an explosion). Simulations 2 and 3 add specific values to the velocities in the velocity equations, i.e. vertical or horizontal single forces to generate P- and S-waves with different dominance with respect to radiation towards the surface. Simulation 2 uses vertical single forces that mainly emit P-waves in vertical direction. Simulation 3 uses horizontal single forces to primarily emit S-waves in vertical direction.

[9] TRM localizes the microtremors to their originating subsurface locations. The particle velocity-time signals of the seismometers (Figures 2b–2d) are time varying boundary values input to TRM. The largest absolute particle velocity (root mean square of the two particle velocity components) at every numerical grid point, which is recorded throughout the entire TRM, is stored at each corresponding grid point.

[10] High particle velocities commonly correspond to high amplitudes of single waves with little geometric spreading or to constructive interference of multiple waves. The latter case occurs most strongly when waves, which are reversely emitted from the seismometer locations, meet each other at their common source location. With a source having an adequate dynamic bandwidth, emitting signals to a sufficient number of seismometers, the source location will stand out due to high particle velocities. As source localization and not signal strength is the primary goal, no geometric spreading correction is required.

[11] Figures 2b, 2c, and 2d show that TRM gives location and roughly microtremor source area for all three simulations. Although the dominant wavelength is about 1000 m (mean P-wave velocity of 3000 m/s and central frequency of

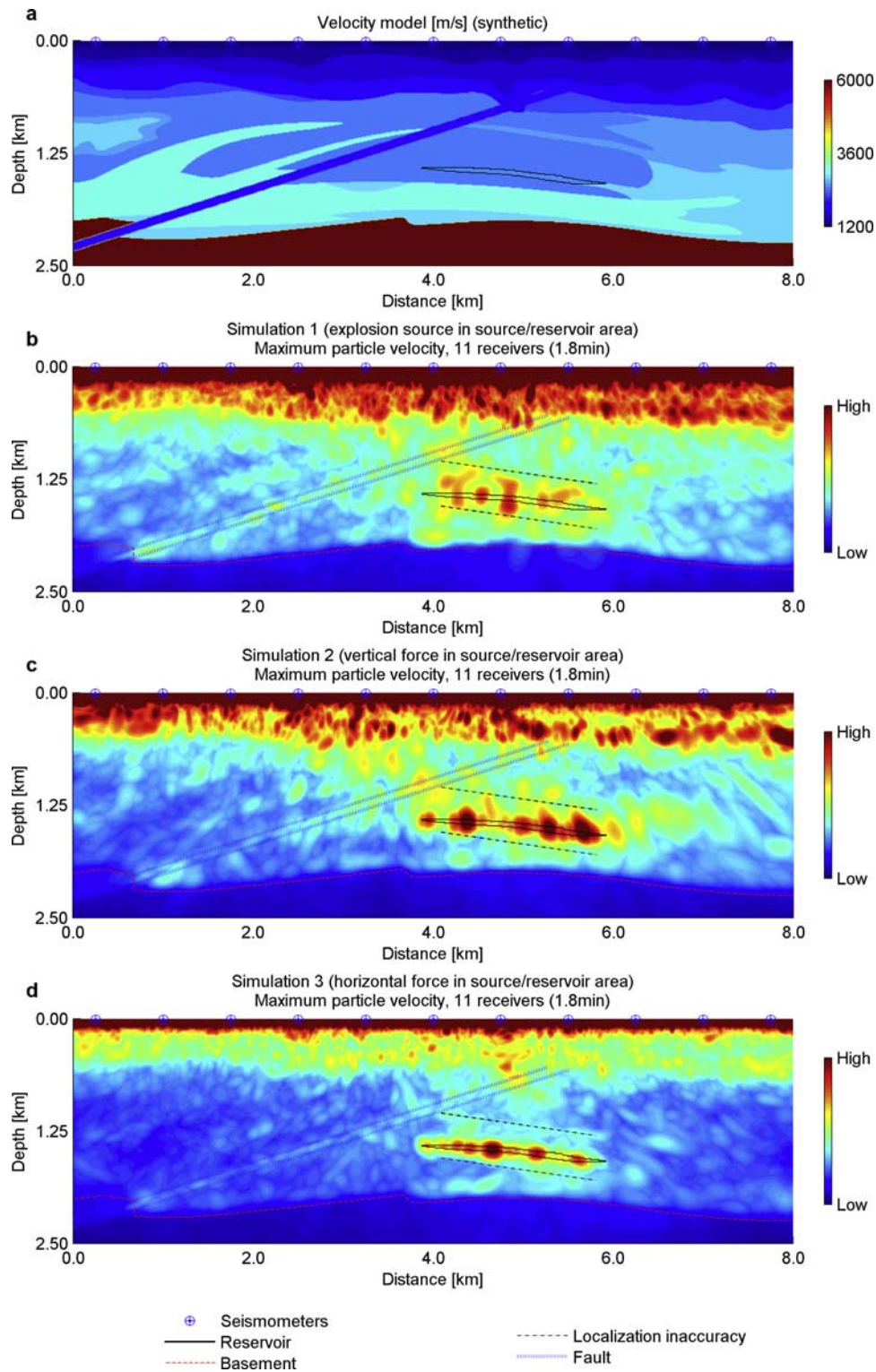


**Figure 2.** (a) The synthetic velocity model consists of ten sediment units and a basement unit. A thin area representing the reservoir defines the seismic source area. (b–d) All time reverse simulations show a focus of high particle velocities in the area of the reservoir, which is the zone of microtremor sources in the forward models.

3 Hz), the source area is located with an adequate accuracy of 250 m or smaller (dashed black lines, Figures 2b–2d).

[12] Localization accuracy depends on whether mainly P-waves or S-waves are emitted in vertical direction. The source area localization in Simulation 1 in Figure 2b (P-wave generation only) shows the lowest accuracy of all three

simulations. P-waves have a longer wavelength than S-waves in the same media so S-waves will be expected to improve the accuracy of source localization. Indeed, Simulation 2 (Figure 2c) shows better localization accuracy. Simulation 3 (Figure 2d) localizes best the source area which now has a clear boundary. Localization accuracy is better in horizontal

than in vertical direction, because the aperture angle is opened upwards toward the seismometers at the surface.

[13] An area adjacent the length of the upper surfaces (Figures 2b–2d) also shows high particle velocities. This is caused by surface waves generated where time reversed velocities are implemented as boundary conditions. Another reason is that geometric spreading has not significantly reduced the high amplitudes of these particle velocities in close vicinity of the seismometers. These reasons indicate detectable microtremor sources may need to be some distance away from the seismometer locations.

### 3. Time Reverse Modeling Applied to Real Microtremors

[14] TRM application for localization of real microtremors uses a velocity profile adapted from conventional seismic surveys and well log data for the study area (Voitsdorf, Austria). TRM applied to real measurements from two low-frequency seismic surveys above reservoirs oil fields in Voitsdorf demonstrates localization of known reservoir subsurface positions.

[15] The two surveys cover parts of the same North-South profile. Both data sets comprise synchronized recordings of seismometers at the surface. Each seismometer records three particle velocity components (vertical, North-South and East-West). The seismometers of Survey 1 cover 1.5 km (Figure 3a) whereas they cover 9 km in Survey 2 (Figure 4a). Survey 1 and Survey 2 profiles overlap where the square within Figure 4a represents the section of Figure 3a.

[16] Only vertical and North-South particle velocity-time signals are input to TRM. Real data processing involves (i) removal of mean deviation, (ii) zero-phase band-pass filtering from 1 Hz to 6 Hz and (iii) resampling of signals on a time array with time intervals corresponding to numerical stability criterion. The seismometers at the right end of Survey 2 are not covered by the velocity model (grid spacing 10 m) so a constant profile extends laterally to the right (Figure 4a).

[17] Figure 3b illustrates high particle velocity result of a TRM application of synthetic microtremor data generated within the known reservoir location. This Survey 1 synthetic forward model uses the real velocity model of Figure 3a and microtremor sources randomly distributed within the reservoir area (ellipse in Figure 3b). These synthetic sources are as in Simulation 2 (Figure 2c) emitting mainly P-waves in vertical direction.

[18] Figures 4b and 4c illustrate maximum particle velocity measurements output from TRM for Survey 2 using two different three minute time intervals of real particle velocity measurements. These two three minute intervals show representative results from a total of 25 different three minute and 2 different 30 minute intervals that have been modeled. Figure 4d illustrates TRM output for the same real microtremor time signals as those of Figure 4b, now band-pass filtered from 10 Hz to 20 Hz.

### 4. Results

[19] TRM of synthetic microtremor data, using either a synthetic or real velocity model, demonstrates accurate subsurface microtremor source localization. Using a veloc-

ity model derived from conventional seismic surveying, good qualitative agreement is found between the position of known hydrocarbon reservoirs (indicated with ellipses in Figures 3c, 4b, and 4c), synthetic microtremor data and real microtremor source localizations from two time separated surveys. Survey 1 microtremor localization results agree with Survey 2 localization results even though the two surveys are separated in time by 16 months and acquisition parameters are different (total number and location of seismometers).

[20] There are high particle velocities between the reservoir and the surface for Survey 1 (Figures 3b and 3c). The high particle velocities above the reservoir in the synthetic simulation (Figure 3b) result from limited aperture caused by relatively small width of the seismometer array. This was verified with simulations having a wider aperture where no high particle velocities were observed above the reservoir. Therefore, the high particle velocities above the reservoir in the real data (Figure 3c) are most likely influenced by limited aperture.

[21] However, high particle velocities are also visible in Survey 2 between the right-most reservoir and the surface (Figures 4b and 4c). These simulations have a much wider aperture than the ones of Survey 1 (Figure 3) and therefore the high particle velocities are caused by additional effects other than limited aperture. The high particle velocities between the reservoir and the surface could result from real microtremor sources (e.g. caused by a leaking of hydrocarbons), from fundamental model uncertainties (e.g. S-wave velocities) or from artifacts due to the projection of 3D signals onto a 2D section.

[22] Because of good qualitative agreement between hydrocarbon reservoir positions, synthetic (Figure 3b) and real Survey 1 (Figure 3c) and Survey 2 (Figures 4b and 4c) microtremor reservoir positions, high particle velocities at the reservoir locations may be true subsurface particle velocity distributions caused by microtremors as opposed to artifacts of numerical modeling and data processing.

[23] TRM using real microtremor data with a 10–20 Hz band-pass filter applied shows that there is no focusing or lensing (and no reservoir indication), indicating that localization due to velocity distribution characteristics of the model is unlikely, since any focusing artifact would also be present for the 10–20 Hz data.

### 5. Conclusions

[24] The numerical simulations show that small underground areas, in which low-frequency microtremors are generated, can be located using TRM. No single event or first arrival time identification is necessary. The characteristics of source radiation significantly influence source localization accuracy. Sources that emit mainly S-waves in vertical direction yield most accurate source localization.

[25] For TRM to localize the source of real microtremors associated with known hydrocarbon reservoirs suggests that low-frequency spectral anomalies measured above reservoirs are generated by signals which originate from within the reservoirs.

[26] Additional studies are needed to address the ambiguity of areas with high particle velocities due to possible low velocity zones or near-surface effects. Also,

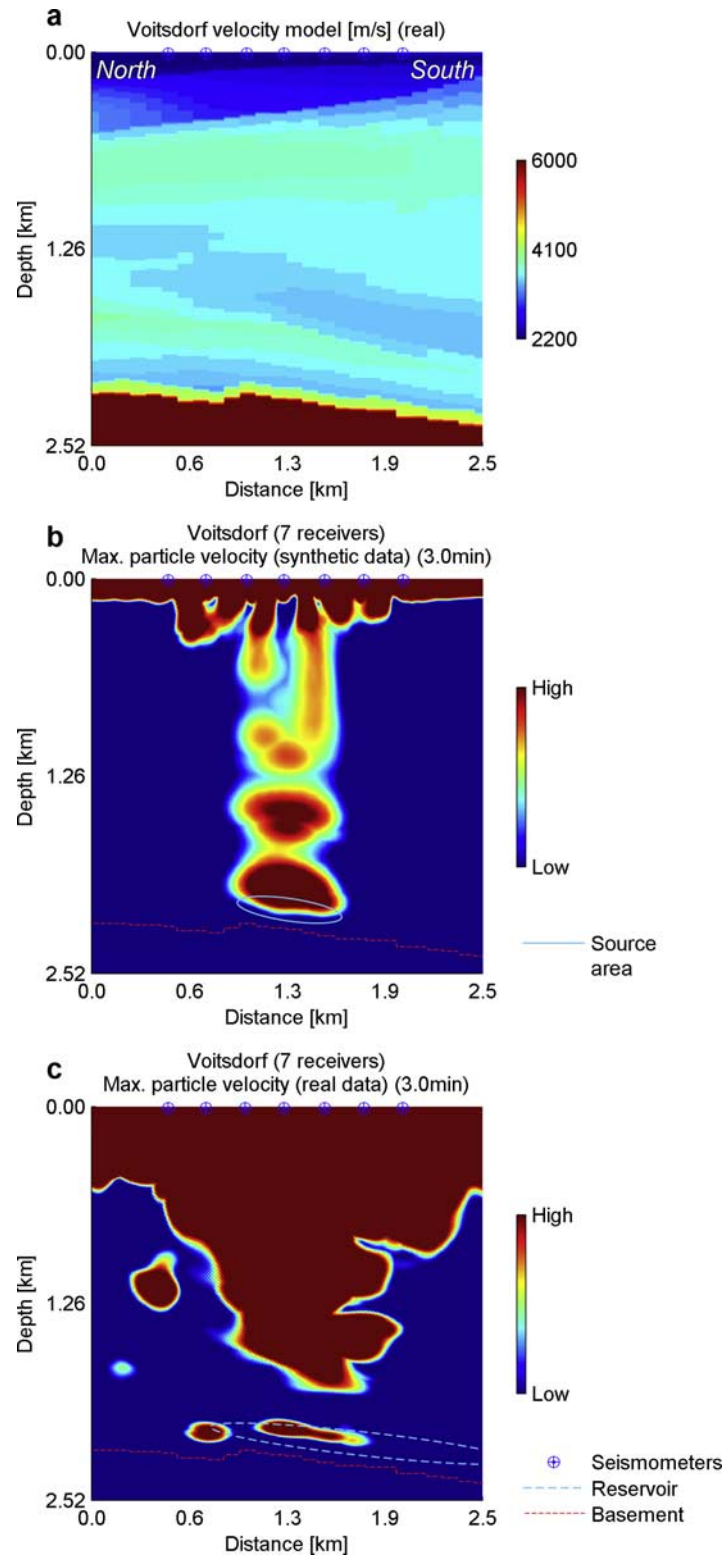


**Figure 3.** (a) The real velocity model of Voitsdorf used for Survey 1 is adapted from conventional seismic surveys and well log data. (b) TRM using synthetic signals with sources within the location of the known reservoir shows that the source location can be identified. (c) TRM with real particle velocities from field measurements shows a particle velocity pattern similar to the synthetic example.

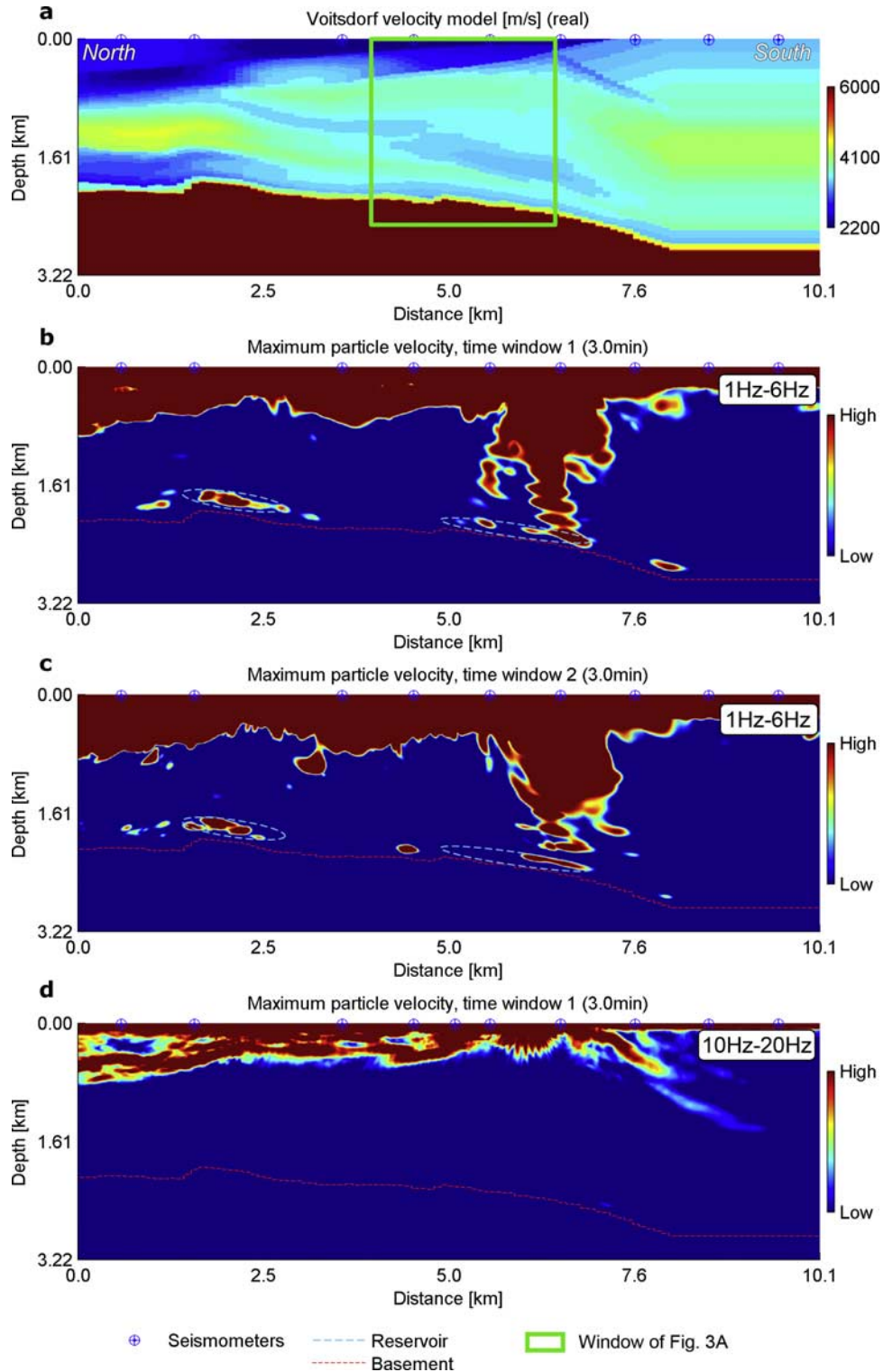


**Figure 4.** (a) The real velocity model of Voitsdorf used for Survey 2 includes the velocity model used in Survey 1 (area bounded with the square is Figure 3a). (b and c) There is a second, known reservoir in the North. TRM of two different time windows, each 3 minutes of real measurements, results in good localization of the reservoirs. (d) TRM of time signals band-pass filtered from 10 Hz to 20 Hz does not show the reservoir location. There are no visible areas of high particle velocities within the basement due to the high P-wave velocity of the basement.

sensitivity of TRM results due to model inaccuracies requires further quantification.

[27] **Acknowledgments.** This work was co-financed by the Commission of Technology and Innovation (CTI) and Spectraseis AG. We thank the Rohoel-Aufsuchungs-Aktiengesellschaft (RAG) for field access and Proseis AG for providing the velocity model. We are grateful to editor Aldo Zollo and to the anonymous reviewer for their thoughtful review.

## References

- Akrawi, K., and G. Bloch (2006), Application of passive seismic (IPDS) surveys in Arabian peninsula, paper presented at Workshop on Passive Seismic: Exploration and Monitoring Applications, Eur. Assoc. of Geosci. and Eng., Dubai, United Arab Emirates, Dec.
- .Claerbout, F. (1968), Synthesis of a layered medium from its acoustic transmission response, *Geophysics*, *33*, 264–269.
- Clayton, R., and B. Engquist (1977), Absorbing boundary-conditions for acoustic and elastic wave-equations, *Bull. Seismol. Soc. Am.*, *67*, 1529–1540.
- Dangel, S., M. E. Shaepman, E. P. Stoll, R. Carniel, O. Barzandji, E.-D. Rode, and J. M. Singer (2003), Phenomenology of tremor-like signals observed over hydrocarbon reservoirs, *J. Volcanol. Geothermal Res.*, *128*, 135–158.
- Fink, M. (1999), Time-reversed acoustics, *Sci. Am.*, *281*, 67–73.
- Gajewski, D., and E. Tessmer (2005), Reverse modelling for seismic event characterization, *Geophys. J. Int.*, *163*, 276–284.
- Garnier, J. (2005), Imaging in randomly layered media by cross-correlating noisy signals, *Multiscale Modeling Simul.*, *4*, 610–640.
- Graf, R., S. M. Schmalholz, Y. Podladchikov, and E. H. Saenger (2007), Passive low frequency spectral analysis: Exploring a new field in geophysics, *World Oil*, *228*, 47–52.
- Kao, H., and S.-J. Shan (2004), The source-scanning algorithm: Mapping the distribution of seismic sources in time and space, *Geophys. J. Int.*, *157*, 589–594.
- Mehta, K., and R. Snieder (2006), Time reversed imaging for perturbed media, *Am. J. Phys.*, *74*, 224–231.
- Saenger, E. H., N. Gold, and S. A. Shapiro (2000), Modeling the propagation of elastic waves using a modified finite-difference grid, *Wave Motion*, *31*, 77–92.
- Schuster, G. T., J. Yu, J. Sheng, and J. Rickett (2004), Interferometric/daylight seismic imaging, *Geophys. J. Int.*, *157*, 838–852.
- Virieux, J. (1986), P-SV-wave propagation in heterogeneous media—Velocity-stress finite-difference method, *Geophysics*, *51*, 889–901.
- Wapenaar, K., J. Thorbecke, and D. Draganov (2004), Relations between reflection and transmission responses of three-dimensional inhomogeneous media, *Geophys. J. Int.*, *156*, 179–194.

---

E. H. Saenger, S. M. Schmalholz, and B. Steiner, Geological Institute, ETH Zurich, Building LEB, D 9, Leonhardstrasse 19, CH-8092 Zurich, Switzerland. (brian.steiner@erdw.ethz.ch)